sustainability

MDPI

Review

Literature Review on the Indoor Air VOCs Purification Performance of Metal–Organic Frameworks

Kaiqiao Wang [1], Jinzhe Nie [1,*], Honghao Huang [1] and Fuqun He [2]

[1] Beijing Key Lab of Heating, Gas Supply, Ventilating and Air Conditioning Engineering, Beijing University of Civil Engineering and Architecture, Beijing 102616, China; wangkaiqiao1@126.com (K.W.); tripleh0711@163.com (H.H.)
[2] Beijing District Heating Group Co., Ltd., Beijing 100028, China; hequn294@163.com
* Correspondence: niejinzhe@bucea.edu.cn

Abstract: Controlling the indoor air (volatile organic compound) VOCs concentration plays an important role in creating a healthy and comfortable living environment. Comparing several VOCs purification measures, solid adsorption is found to be a promising air cleaning method for civil buildings, which have diverse VOCs pollutants. For solid adsorption technology, absorbance is the key to its air-cleaning performance. Compared with traditional adsorbent materials, (metal–organic frameworks) MOFs have excellent physical parameters and are promising adsorbent materials. In this paper, the synthesis and adsorption mechanisms underlying several metal–organic frameworks are summarized. The exploration and experiment measurements of VOCs adsorption performance according to the metal–organic frameworks are summarized. The exploration of these materials' stability during air cleaning is reviewed. Finally, some application examples of metal–organic frameworks for VOCs adsorption are given. This literature review demonstrates that metal–organic frameworks can be promising adsorbents for indoor air cleaning. The green synthesis methods, stability, adsorption performance under low concentration and diverse VOCs conditions, and application methods for metal–organic frameworks should be further researched before their large-scale application.

Keywords: metal–organic frameworks; VOCs; solid adsorption; adsorption mechanism; stability

Citation: Wang, K.; Nie, J.; Huang, H.; He, F. Literature Review on the Indoor Air VOCs Purification Performance of Metal–Organic Frameworks. *Sustainability* **2023**, *15*, 12923. https://doi.org/10.3390/su151712923

Academic Editors: Ying Sheng and Chunxiao Su

Received: 17 July 2023
Revised: 21 August 2023
Accepted: 23 August 2023
Published: 27 August 2023

1. Introduction

It has been found that most urban residents in China spend 80% of their lives indoors [1]. According to the results of interviews conducted by Professor NEIL E. KLEPEIS's team [2] with tens of thousands of respondents of all ages across the United States, they spend approximately 87% of their day in a room and 6% in a closed car. Women and children [3,4] represent a more vulnerable group that spends more time indoors. Therefore, the quality of indoor air seriously affects the level of human health, and the study of indoor air quality has become an important topic. Among the various indicators used to evaluate air quality, the concentration of volatile organic compounds (VOCs) has paramount importance.

1.1. Sources of VOCs

The advancement of science and technology and the refinement of human aesthetic preferences have led to a proliferation of diverse interior decorations, decoration materials, and furniture. However, a consequential issue arises from the increased utilization of chemical additives in these items, resulting in elevated concentrations of indoor VOCs [5]. VOCs are able to volatilize at ambient temperatures. According to the WHO [6], VOCs encompass organic compounds with boiling points ranging from 50 °C to 260 °C and saturated vapor pressures surpassing 133.32 Pa at room temperature. In adherence with the Chinese standard GB/T18883-2022, titled "Indoor Air Quality Standards," the collective term "total volatile organic compounds" (TVOCs) is defined as volatile compounds having retention times between hexane and n-hexadecane, as ascertained using Tenax TA or

analogous adsorption tube sampling methods and subsequent analysis using non-polar or weakly polar capillary columns with a polarity index below 10. The Chinese specification GB55016-2021, titled "General Specification for the Built Environment," prescribes explicit regulations for various VOCs and TVOC content, as presented in Table 1. While the external environment does impact indoor VOCs levels [7], indoor activities exert a more direct influence, such as indoor smoking, cooking activities [8], household appliance usage, renovation procedures, and the application of cosmetic products [9]. Table 2 illustrates select indoor sources of VOCs [10].

Table 1. GB55016-2021 indoor air pollutant concentration limits.

Pollutants	Class I Civil Construction	Class II Civil Construction
Formaldehyde (Bq/m^3)	≤0.07	≤0.08
Benzene (mg/m^3)	≤0.06	≤0.09
Toluene (mg/m^3)	≤0.15	≤0.20
Xylene (mg/m^3)	≤0.20	≤0.20
TVOC (mg/m^3)	≤0.45	≤0.50

Table 2. Indoor sources of VOCs.

VOCs Classification	VOCs	Examples of Household Products
alcohols	3-octanol, 2-ethyl alcohol	aerosols, window cleaners, paints, paint thinners, cosmetics, and adhesives
aldehydes	acetaldehyde	plastics, paints, foam insulation, glues, deodorants, fuels, hair dryers, cell phones, televisions, radiators, incense, irons, chargers, and tobacco smoke
	formaldehyde	pressed wood products (plywood wallboard, particle board, and fiberboard), treated wood, foam insulation, water-based coatings, combustion sources, tobacco smoke, upholstered furniture, furniture fillers, carpets, durable pressed draperies, other textiles, glues/adhesives, cosmetics, cleaners, markers, ballpoint and pen inks, and dyes
aromatics	benzene	tobacco smoke, paints, degreasers, adhesives, adhesive removers, home heating oils, home ovens, incense, molding waxes, displays, and plastics
	toluene	fuel oil, paints, paint thinners, lacquer, adhesives, coatings, nail polish, furniture polish, shoe polish, monitors, televisions, irons, decorative lamps, cell phones, rechargeable batteries, printed matter, incense, exotic wood products, beads, cleaners, detergents, and cigarettes
	xylene	fuel oil, paints, paint thinners, degreasers, lubricants, waterproofing, plastics, synthetic rubber, polyester clothing, pesticides, cleaners, monitors, computers, chargers, game consoles, ovens, decorative lamps, hair dryers, cell phones, televisions, rechargeable batteries, printing materials, incense, beads, Christmas sprays, and tobacco smoke

1.2. Hazards of VOCs

The adsorption of VOCs by the human body elicits a cascade of adverse physiological responses, encompassing symptoms such as nausea, headaches, discomfort of mucosal tissues, and even the potential for fatality [11,12]. Acetaldehyde can irritate the eyes, skin, and respiratory tract, increase the risk of cancer, and can cause paralysis or even death at high concentrations. Toluene and xylene, at elevated levels, can induce central nervous system anesthesia, presenting mild symptoms including dizziness, headaches, nausea, and chest tightness, while severe cases may manifest as respiratory failure. Benzene and toluene have been confirmed to be carcinogenic [13]. Zhao et al. revealed that exposure to VOCs induces alterations in the gas–liquid surface properties of lung surfactants, causing a great potential for pulmonary pathology [14]. Notably, in certain samples collected from France, it was observed that elderly people exposed to indoor VOCs had a significantly

increased risk of respiratory diseases such as asthma and rhinitis [4,15,16]. Furthermore, a study conducted in Baotou, China, involving 140 randomly selected samples from a pool of 5000 questionnaires, demonstrated a statistically significant association between VOCs and the incidence of eczema in newborns [17].

1.3. Means for VOCs Removal

The means for VOCs removal include physical and chemical adsorption, catalysis, biotechnology, plasma gas, membrane separation technology, and condensation technology [18].

Catalytic oxidation technology has proven to be one of the most reliable post-treatment technologies for VOCs emissions, with high efficiency and good economy. Precious metal catalysts have excellent results for formaldehyde removal, but their main application is in the treatment of industrial exhausts. Therefore, further investigation is warranted to ascertain their effectiveness in indoor environments [19]. Plasma gas is a technology that uses electrical energy to drive the degradation of VOCs, but it is limited by the energy input and the generation of secondary products, and the technology needs to be further developed [20]. Biological technology includes the use of biofilters or green plants to remove VOCs and produce harmless by-products. Studies have proven its effectiveness for formaldehyde, benzene, toluene, and xylene removal, but the removal time is relatively long, the biofilters need to be dried, and there are large differences between adsorption plants [21,22]. Condensation technology entails the regulation of temperature and pressure to condense VOCs, subsequently discharging them through pipelines. However, the condensation system and piping design are complicated because the condensation conditions of VOCs are different, and better design solutions and technologies are needed to optimize the overall system and reduce the cost [23–25]. Membrane separation technology entails the utilization of membranes for the screening, enrichment, and subsequent removal of VOCs. Primarily applied in industrial production settings, this technology faces challenges such as insufficient membrane stability and the inability to concurrently treat and recover multiple VOCs [26]. Physical adsorption primarily relies on intermolecular van der Waals forces or hydrogen bonding, whereas chemisorption relies on the formation of chemical bonds between the adsorbent and adsorbate molecules. Adsorption technology is simpler and does not produce by-products in the purification process, but the requirements for adsorbent materials are relatively high [27]. Currently, adsorption serves as the prevailing method for VOCs removal in civil buildings. Commonly used adsorption materials include silica gel, activated carbon, molecular sieve, zeolite, and metal–organic frameworks (MOFs). These materials are effectively used in solid air conditioners, such as fixed beds and wheels, to achieve efficient air purification. In the realm of adsorption materials, physical characteristics, encompassing specific surface area, pore size, and pore volume, exert a crucial influence on the adsorption efficacy. MOFs, as novel adsorbent materials, exhibit superior physical characteristic parameters compared with traditional counterparts, offering increased potential for modification and presenting promising avenues for further research [28–30].

Currently, MOFs are not utilized or produced on a large scale like traditional adsorbent materials, and more products and applications exist at the laboratory stage. The origin of the raw materials and the synthesis methods used vary from laboratory to laboratory, resulting in differences in physical characterization parameters even for the same MOFs. In this paper, we collected some characterization data for MOFs and conventional materials, please see Table 3.

Table 3. Characterization parameters of MOFs.

Material	S_{BET} m^2/g	$S_{Langmuir}$ m^2/g	Pore Volume cm^3/g	Reference
MOF-199	1237	1591	0.47	[29]
MOF-5	424	535	0.22	[29]
ZIF-67	1401	1211	1.22	[29]
Ni-MOF-74	882	-	0.385	[31]
Mg-MOF-74	1174	-	0.556	[31]
CPO-27-Zn	979	-	0.28	[32]
CPO-27-Co	1083	-	0.36	[32]
CPO-27-Ni	1113	-	0.39	[32]
MIL-101(Cr)	3367	-	2.35	[33]
Cu-3@MIL-101(Cr)	2518	-	1.55	[33]
MIL-100(Fe)	1398.7	-	1.085	[34]
MIL-101(Fe)	873.3	-	0.737	[34]
MIL-53(Fe)	268.6	-	0.338	[34]
UiO-66-NH_2	568	765	0.36	[35]
C-U-N-0.5	795	978	0.39	[35]
UiO-66(Zr)	1300	-	1.65	[36]
Ga-MIL-53	560	-	-	[37]
MIL-101	2367	-	1.48	[38]
MOF-199	1212	-	0.46	[39]
UiO-66-NH_2	963	-	0.58	[39]
HKUST-1	1400	-	0.56	[40]
Fe-HK-2	1707	-	0.93	[40]
HKUST-1	1568.5	2081.4	0.75	[41]
MOF-177	2970	4170	1.11	[42]
MOF-47	755	-	0.28	[43]
MIL-125-NH_4	1450	-	0.61	[43]
MIL-140B	420	-	0.17	[43]
Silica gels A	756	-	0.45	[44]
Silica gels B	514	-	0.76	[44]
Silica gels	766	-	0.44	[45]
Zeolite-HMOR	270	-	0.087	[46]
Zeolite-NMOR	332	-	0.162	[46]
Zeolite-MS13X	582	-	0.215	[46]
Zeolite-HY5.6	650	-	0.228	[46]
Zeolite-HY4.8	663	-	0.284	[46]
Zeolite-HY901	591	-	0.298	[46]
DAY zeolite	704	-	0.268	[47]
AC	1084	-	0.63	[48]
AC	786	-	0.33	[49]

1.4. Summary

This section summarizes the definitions of VOCs, some of the sources of VOCs, and the hazards of VOCs to humans as established by national or international organizations. Among the main means for VOCs removal at present, various catalytic technologies are prone to producing harmful by-products. Adsorption technology hardly produces by-products and is currently the most applicable purification means for residential buildings. For adsorption technology, the key point is the adsorption material. Advancements in adsorption materials play a critical role in substantially augmenting the efficiency of adsorption and purification processes.

2. Synthesis and Adsorption Mechanism of MOFs

2.1. Synthesis of MOFs

The synthesis of materials involves chemical reactions that necessitate energy transformations. Consequently, the provision of energy becomes a crucial aspect of material synthesis. The energy source, its duration, and the reaction environment collectively in-

fluence the reaction process, while varying parameters and diverse methodologies exert distinct effects on the resulting material characteristics, such as specific surface area, pore volume, and pore size distribution [50].

2.1.1. Hydrothermal Approach

Over the past three decades, the hydrothermal method has emerged as a prominent synthesis approach for the development of MOFs. This technique entails the combination of inorganic salt solvents and organic ligands within a sealed vessel, allowing the materials to amalgamate and precipitate into crystals using controlled heating. Building upon this fundamental principle, scientists have successfully synthesized renowned MOFs series, such as MIL, UIO, and PCN [51]. Colin McKinstry's team [52] produced MOF-5 using the continuous hydrothermal method to increase the output efficiency by up to 1000 $kg/m^3/day$. To address the issue of undesirable polycrystalline and amorphous product formation resulting from uncontrolled in situ generation during material synthesis, Dawei Feng's team proposed a dynamic size-enhanced synthesis method using preformed inorganic building blocks. This methodology effectively preserves the integrity of material metal clusters, resulting in more robust MOFs structures [53]. The experimental findings of Franck Millange's team [54] and Enrica Biemmi's team [55] emphasize the critical significance of temperature and duration control in the hydrothermal method. Temperature exerts a substantial impact on material purity, whereas excessively prolonged heating times can detrimentally affect material integrity and performance. Consequently, precise control of these parameters is essential to ensure desirable material properties and synthesis outcomes.

2.1.2. Microwave Synthesis Method

The microwave synthesis method utilizes microwaves to introduce radiation energy, which can effectively reduce the reaction time, control the material properties, and distinguish between the material and its by-products [56]. Reza Vakili's team [57] used the microwave synthesis method instead of the hydrothermal method to synthesize UIO-67, and the results showed that the synthesis time was significantly reduced from 24 h to 2–2.5 h, and the adsorption experiments using CO_2 and CH_4 proved that the adsorption amount did not decrease. Xiaofei Wu's team [31] compared the preparation of Ni-MOF-74 and Mg-MOF-74 using the microwave and hydrothermal methods and found that Ni-MOF-74 S_{BET} increased from 882 m^2/g to 1252 m^2/g and Mg-MOF-74 S_{BET} increased from 1174 m^2/g to 1416 m^2/g. The micropore volume of Ni-MOF-74 increased from 0.385 cm^3/g to 0.564 cm^3/g, and the micropore volume of Mg-MOF-74 increased from 0.556 cm^3/g to 0.682 cm^3/g. The reaction time was shortened from 24 h to 100 min, and the adsorption capacity slightly increased.

2.1.3. Ultrasonic Synthesis Method

Ultrasonic technology utilizes ultrasonic waves during the reaction process. The ultrasonic waves cause the reactants to produce localized and instantaneous high pressure and heat, thereby accelerating the reaction [58]. Enamul Haque and his team compared the effects of electrical heating and ultrasonic technology at lower temperatures ($\leq$80 °C) on MIL-53(Fe). In the experiments, they found that ultrasonic technology can achieve nucleation rates up to 50 times greater than that of electric heating. Furthermore, they found that ultrasonic technology can cause crystallization efficiencies up to hundreds of times higher. Based on the calculations of the reaction, the researchers determined that the introduction of ultrasonic increased the pre-exponential factors, and so accelerated the reaction [59]. In the team's study investigating the ultrasonic synthesis of COP-27, they concluded that the reaction rate achieved using ultrasonic irradiation exceeded that of conventional electrical heating. Materials produced under ultrasonic conditions exhibited maximal porosity and minimal crystal size. Conversely, materials obtained using electrical heating demonstrated lower porosities and larger crystal sizes [32].

2.1.4. Electrochemical Synthesis

Electrochemical synthesis utilizes the energy transfer of electrical and chemical energy in the reaction. The addition of voltage has been demonstrated as an effective approach for promoting the growth of functional MOFs coatings, thus serving as a vital method for obtaining MOFs crystals [60]. Additionally, the strength of the electric current and the duration of the reaction have emerged as crucial factors influencing the efficiency and purity of material production. Notably, in the experimental investigations conducted by Otávio José de Lima Neto's team [61], it was observed that the electrochemical method significantly reduced the reaction time in comparison with the hydrothermal method, highlighting the efficacy and time-saving potential of this approach. Kasra Pirzadeh's team [62] synthesized $Cu_3(BTC)_2$ using electrochemical synthesis (S_{BET} = 1474.1 m^2/g, pore volume = 0.62 cm^3/g), which showed a slight increase in specific surface area and pore volume compared with other synthesis methods and had good thermal stability and high crystallinity. It performed well in adsorption experiments using CO_2 and CH_4, and there was no decrease in the adsorption amount after six cycles in the cyclic adsorption experiments on CO_2.

2.1.5. Mechanochemical Synthesis

During the mechanochemical synthesis method, the reaction takes place with mechanical grinding under the condition of a small amount of solvent, so it produces less waste liquid. This type of synthesis generally does not require heating, so it also saves energy [63]. Daofei Lv's team [64] proposed an efficient mechanochemical synthesis method, which included grinding for 60 min to obtain good crystallinity with a maximum S_{BET} = 3465.9 m^2/g. The adsorption capacity of the prepared material for alkanes was verified to be stronger than that for conventional adsorption materials using adsorption experiments. Yongwei Chen's team [65] obtained MOF-505-K with S_{BET} = 977 m^2/g using liquid-assisted mechanochemical synthesis, and their experiments proved that the material had good selectivity for CO_2 and provided material options for CO_2 collection.

2.2. Mechanism Underlying MOFs Adsorption

Studying the MOFs adsorption mechanism helps to understand the microscopic world of MOFs and plays an important role in the research work on synthesizing and modifying materials. In addition to the van der Waals force, extensive research has led to the categorization of MOFs adsorption mechanisms into several distinct classifications, encompassing metal site adsorption, π-bond adsorption, hydrogen bond adsorption, electrostatic force adsorption, acid–base interactions, and the breathing behavior of MOFs [66].

2.2.1. Metal Site Adsorption

Chan-Yuan Huang's team [67] investigated the adsorption properties of MIL-101 (S_{BET} = 736 m^2/g, pore volume = 1.5 cm^3/g) for six VOCs at atmospheric pressure using a quartz crystal microbalance (Figure 1). They verified the strong affinity of metal sites for heteroatomic VOCs. Dongfang Wang's team [33] investigated the adsorption properties of MIL-101(Cr) (S_{BET} = 3367 m^2/g, pore volume = 2.35 cm^3/g) copper doping experiments to synthesize Cu-3@MIL-101(Cr) (S_{BET} = 2518 m^2/g, pore volume = 1.55 cm^3/g). Despite a decrease in specific surface area and pore volume, the introduction of additional metal sites in the material resulted in an increased maximum adsorption capacity for benzene, elevating it from 103.4 mg/g to 114.4 mg/g. Kumar Vikrant's team [68] conducted experiments and simulations on the adsorption of Cu-MOF-199, Co-CUK-1, Zr-(UiO-66), and UiO-66-NH_2 with eight mixed VOCs. The findings revealed that Cu-MOF-199 exhibited commendable adsorption capacities for all VOCs types, with unsaturated metal sites playing a crucial role. In a study by Feng-Ji Ma's team [69], $Cu_3(BTC)_2$ was combined with polymetallic oxides, and the incorporation of alkali metal ions facilitated the introduction of additional unsaturated metal sites. Adsorption experiments on VOCs confirmed that the interaction between alkali metal cations and the adsorbent resulted in enhanced adsorption performance.

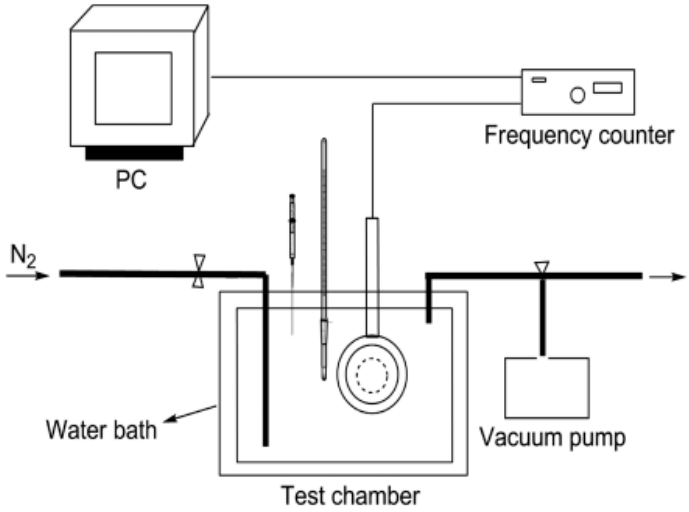

Figure 1. Quartz crystal microbalance system [67].

2.2.2. π-Bond Adsorption

Xiaoling Ma's team [34] tested the adsorption of MIL-100(Fe) on toluene, and the main adsorption mechanism was found to be the π-π bond formed between the organism and the benzene ring, as shown using X-ray photoelectron spectroscopy analysis. Philippe Trens' team [70] performed a study using MIL-101(Cr) (Figure 2) adsorption experiments and simulations on n-hexane and benzene vapor and confirmed that the π-π-bond formation contributes to the adsorption of benzene by the material. In the competitive adsorption of hexane and benzene, hexane inhibits π-bond stacking to some extent to reduce the adsorption of benzene. The team of Kowsalya Vellingiri [71] studied the adsorption of 14 volatile or semi-volatile organics by MOF-5, Eu-MOF, and MOF-199, and their DFT simulations showed where π-π bonding is a key factor affecting the adsorption performance. The configuration of the adsorption apparatus is depicted in Figure 3. The team of Chongxiong Duan [72] optimized the synthesis of MIL-100(Fe) to synthesize the MIL-100(Fe)_An series, and they similarly used adsorption density simulations to show that the stacking of π-π bonds plays an important role in the adsorption of toluene. The experiments conducted by Vipin K. Saini's team [73] clearly showed that MOF-199 adsorbs more benzene than n-hexane and cyclohexane, which is also due to the ease of formation of π-bonds between the metal sites in the material and benzene.

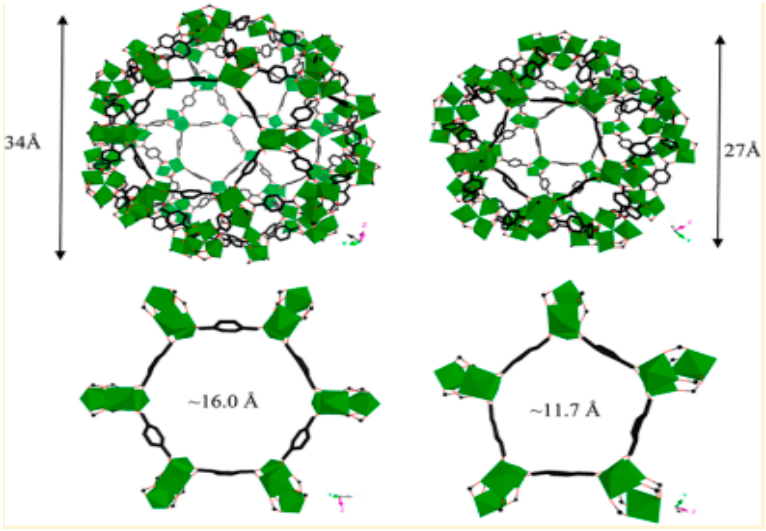

Figure 2. Structure of MIL-101(Cr) [70].

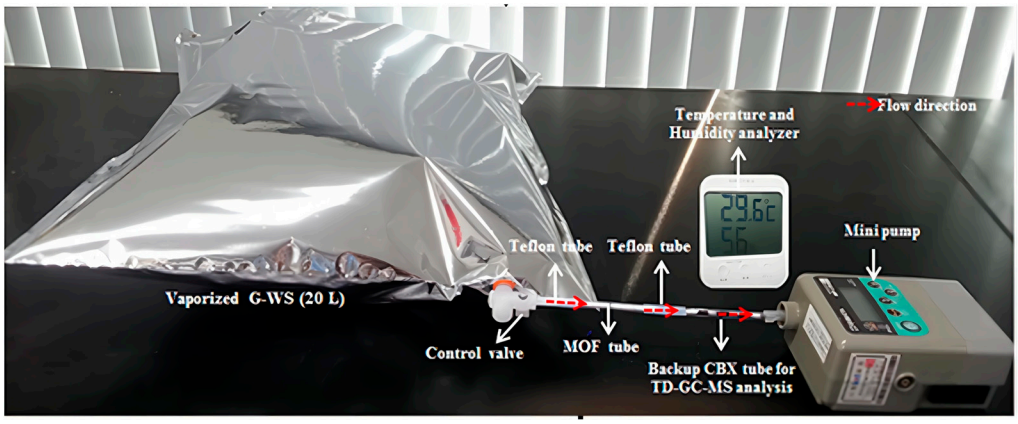

Figure 3. MOFs adsorption device system diagram [71].

2.2.3. Hydrogen Bonding Adsorption

Wang et al. synthesized α-CD-MOF-K, β-CD-MOF-K, and γ-CD-MOF-K to investigate the adsorption of formaldehyde vapor by MOFs at 293 K and 1 atm (Figure 4). Among the frameworks, γ-CD-MOF-K exhibited optimal adsorption performance with a maximum adsorption capacity of 36.71 mg/g, which is approximately nine times higher than that of activated carbon, a conventional adsorbent. The researchers determined the elevated formaldehyde adsorption capacity of this MOFs was predominantly attributed to the influence of hydrogen bonding [74]. Using experiments and simulations, Maria Inês Severino's team [75] showed that mesoporous or microporous MOFs with enough open metal sites, such as MIL-100(Fe), can also capture polar VOCs molecules well in humid environments due to the formation of hydrogen bonds. It is not only the presence and number of hydrogen bonds that affect the adsorption performance, but the acidity and alkalinity of hydrogen bonds are also factors to be considered [76].

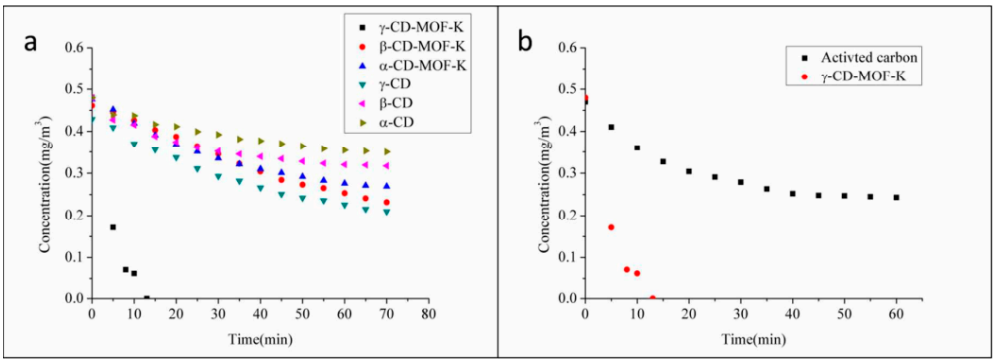

Figure 4. (**a**) The concentration of formaldehyde changes due to the adsorption of α-CD-MOF-K, β-CD-MOF-K, γ−CD-MOF-K, α-CD, β-CD and γ-CD. (**b**) Comparison of adsorption properties of activated carbon and γ-CD-MOF-K [74].

2.2.4. Electrostatic Force Adsorption

Ying Wu's team [77] compared IRMOF-1 and IRMOF-NH_2 in the adsorption of VOCs and found that the addition of the -NH_2 group caused electron transfer of the material, changing the electrostatic density of the material and increasing some atomic charges. It is also reasonably speculated that the adsorption ability of the material to methanol is enhanced due to the electron-giving effect of the amino group. The incorporation of carbonaceous material enhances the electrostatic force of the material, and the adsorption of CCL_4 by MIL-101 is 2059 mg/g under conventional conditions, and MIL-101/GO adsorption is enhanced to 2368 mg/g [78].

2.2.5. Breathing Behaviors

The flexible structure of MOFs gives rise to a unique respiratory effect, just like the breathing behaviors of a living creature. Some reversible structural changes occur when external stimuli are changed, e.g., pore size changes cause the material to release or absorb substances [79].

2.3. Summary

The means of synthesis is an important way to be able to use MOFs on a large scale, and more advanced and reasonable means of synthesis can improve the efficiency and quality of synthesis. In this section, we describe how researchers in various laboratories have tried various methods to change the means of energy introduction and add auxiliary techniques to reduce the synthesis time and increase the stability of synthesis. In order to scientifically improve the synthesis and enhance the performance of the materials, it is necessary to understand the basic mechanism of adsorption and make corresponding improvements. Different adsorbents have different adsorption mechanisms for different VOCs, and some of the literature surveyed is organized in this section, as shown in Table 4.

Table 4. Adsorption mechanisms of different adsorbents to pollutants.

MOFs	VOCs	Adsorption Mechanism	Reference
MIL-101(Cr)	n-hexane, toluene, methanol, butanone, dichloromethane, n-butylamine	metal site adsorption	[67]
Cu-3@MIL-101	benzene	metal site adsorption	[33]
Cu-MOF-199	benzene, toluene, styrene, m-xylene, methyl ethyl ketone, methyl isobutyl ketone, butyl acetate, isobutanol	metal site adsorption	[68]
$Cu_3(BTC)_2$	cyclohexane, benzene, and toluene	metal site adsorption	[69]
MIL-100(Fe)	toluene	π-bond adsorption	[34]
MIL-101(Cr)	hexane, benzene	π-bond adsorption	[70]
MOF-5, Eu-MOF, MOF-199	benzene	π-bond adsorption	[71]
MIL-100(Fe)	toluene	π-bond adsorption	[72]
γ-CD-MOF-K	formaldehyde	hydrogen bonding adsorption	[74]
MIL-101/GO	CCL_4	hydrogen bonding adsorption	[78]

3. VOCs Adsorption by MOFs

In 1995, Professor Yaghi of Arizona State University first named a unique porous material as a metal–organic framework; since then, this material has gradually come into the limelight and ushered in a new era of porous materials [80,81]. This unique porous material is nowadays used in various fields such as gas storage and capture, catalysts, drug production, etc. In a report from 2001, Prof. Yaghi's team found that the storage capacity and safety of MOFs for methane exceeded that of some zeolite materials, proving the great potential of MOFs for gas adsorption [82].

3.1. Adsorption Performance

In order to better apply MOFs in adsorption apparatuses, it is necessary to understand the adsorption capacity of the materials on VOCs and their application scenarios.

3.1.1. Toluene Adsorption

Xiaoling Ma's team [34] conducted toluene adsorption experiments (Figure 5) on three iron-based MOFs synthesized using the hydrothermal method. The maximum toluene adsorption capacity of the three materials MIL-100(Fe), MIL-101(Fe), and MIL-53(Fe) were 663, 180, and 114 mg/g, respectively, in static pure toluene vapor adsorption. In dynamic adsorption, toluene gas with a concentration of 1400 mg/m^3 was prepared with synthetic air at a flow rate of 79% N_2 and 21% O_2 as the carrier gas and blown through gas at a flow rate of 1000 mL/min. When the concentration of toluene gas was changed to 1100, 1400, 1600, or 1900 mg/m^3, the maximum saturation adsorption capacity of MIL-100(Fe) was obtained as 188.6, 214.1, 247.9 and 271 mg/g, respectively. Xiaoyu Shi's team [35] conducted modification experiments on UiO-66-NH_2 with different molar ratios (0.3, 0.5, 1) of CTAB/Zr4+ to obtain UiO-66-NH_2, C-U-N-0.3, C-U-N-0.5, and C-U-N-1. By testing the maximum adsorption of UiO-66-NH_2 and C-U-N-0.5, which have large specific surface area, at 298k, 323k, 348k, and 373k with 7 mL/min argon as a carrier gas carrying 1000 ppm toluene in a 50 mL/min mixture of dynamic adsorption, respectively, we obtained 162, 145, 95, and 28 mg/g and 228, 57, 35, and 28 mg/g. Chongxiong Duan's team [83] adjusted the microporous material to mesoporous material by changing the synthetic synthesis method, adjusting the ratio of water/ethanol, and the number and type of templates during the synthesis of CU-BTC to obtain C-CU-BTC, CU-BTC_HC (H = 1, 2, 3, 4) S_{BET} = 1309, 950, 974, 937, 793 m^2/g, and D_{meso} = 1.84, 3.61, 3.82, 4.29, 4.89 nm. It was also verified that the modified material increased the toluene adsorption capacity by 20% due to its mesoporous structure. The Ky Vo team [36] prepared mixed ligand UiO-66(Zr) structures using the microwave-assisted continuous flow method to improve the material production efficiency and obtained UiO-66(Zr), UiO-66(Zr)-NH_2-25, UiO-66(Zr)-NH_2-50, UiO-66(Zr)-NH_2-75, and UiO-66(Zr)-NH_2-25, with measured S_{BET} = 1300, 1082, 1061, 956, and 935 m^2/g and production efficiencies of 6.5, 6.8, 7.2, 7.7, and 8.2 g/h, respectively. The toluene adsorption capacity of a sample was tested by passing a test gas of 99.99% toluene gas and 1000 ppm air at a flow rate of 0.3 L/min through a fixed bed with 0.2 g of sample. The adsorption capacity of the prepared UiO-66(Zr) for toluene was comparable to that made using the conventional method; when NH_2 was added, the adsorption capacity was significantly increased.

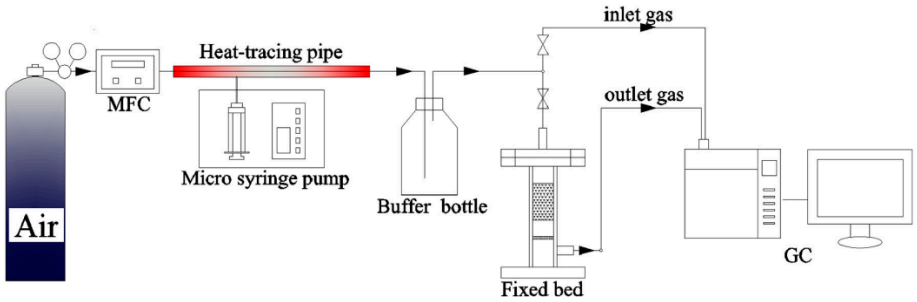

Figure 5. VOCs dynamic adsorption system [34].

3.1.2. Formaldehyde Adsorption

Wei-Qin Xu's team [84] modified MOFs with Cu elements to obtain Cu-MOF. The adsorption capacity of 300 ppm formaldehyde was investigated using the thermogravimetric method, and good enrichment capacity was found. Jean-Pierre Bellat's team [37] compared the adsorption capacity of zeolite, mesoporous silica, activated carbon, and Ga-MIL-53 (S_{BET} = 560 m^2/g) for the adsorption capacity of formaldehyde (Figure 6). Because of the breathing behavior, the adsorption of Ga-MIL-53 spiked between 0.4 hpa and 0.7 hpa, and the adsorption of MOFs was less than several other adsorbent materials in the low-pressure range. Zhong Wang's team [38] modified MIL-101 with ethylene diamine (ED) to improve its adsorption capacity and recyclability. The specific surface areas of MIL-101, ed -MIL-101(Cr)-1, and ed -MIL-101(Cr)-3 were 2367, 764, and 382 m^2/g, and the pore volumes were 1.48, 0.58, and 0.34 cm^3/g, respectively.

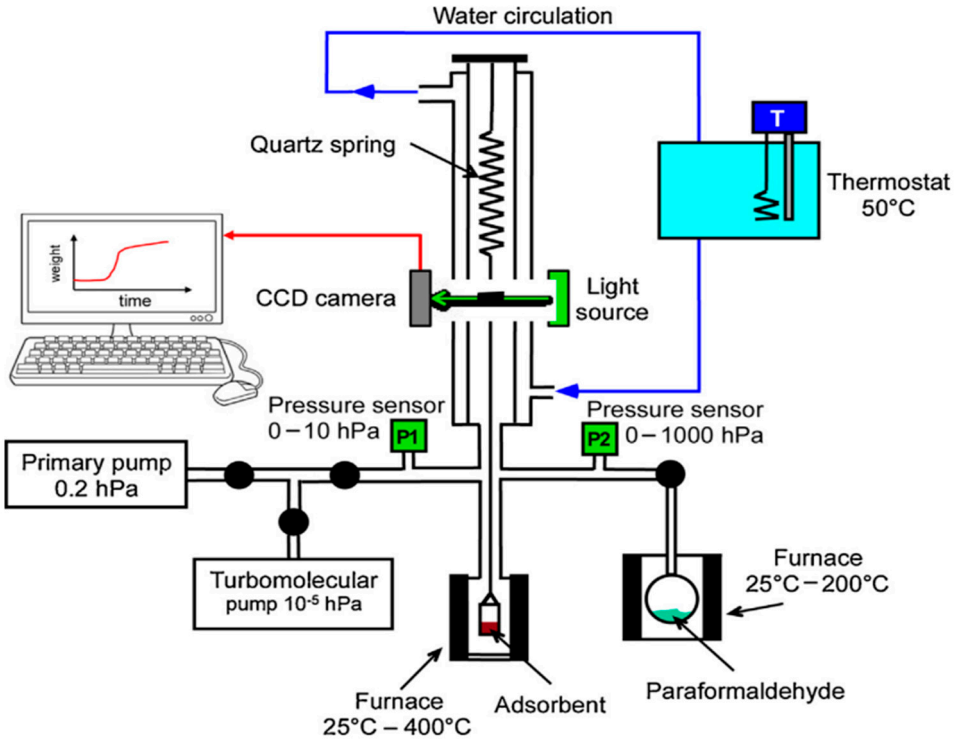

Figure 6. The system for measuring the adsorption isotherms of gaseous formaldehyde [37].

3.1.3. Benzene Adsorption

Chenpeng Wang's team [85] used MOF-199 as a blueprint, carbonized it with glucose at 500, 700, and 900 °C, and then modified it with KOH to obtain the MC-T-n series (T is the carbonization temperature, and n is the KOH to sample mass ratio). The series included MC-500, MC-700, MC-900, MC-500-6, MC-500-4, MC-500-3, MC-700-3, and MC-900-3 with S_{BET} = 379, 421, 583, 2320, 2149, 2033, 1400, and 1064 m^2/g and pore volume = 0.23, 0.25, 0.33, 1.05, 0.02, 0.95, 0.69, and 0.58 cm^3/g, respectively. Among them, MC-500-6, which had the highest specific surface area and pore volume, adsorbed 12.8 mmol/g of benzene vapor at 25 °C, which was twice the adsorption capacity of unmodified MOF-199 and 2–11 times that of conventional adsorbent materials. The heat of adsorption study demonstrated that the adsorption of benzene vapors by the modified sample was greater than that of water adsorption. Botao Liu's team [39] prepared MOF-199 and UiO-66-NH_2 using the hydrothermal method with S_{BET} = 1212, 963 m^2/g and pore volume = 0.46, 0.58 cm^3/g, respectively, and studied the materials using the penetration method at different relative humidity (RH = 0%, 20%, 50%, 80%, and 100%) to benzene (10, 50, 100, and 200 ppm). The results showed that the adsorption at RH = 0% was significantly greater than that with RH, probably due to the following: (1) the materials are more selective for water than benzene, (2) the adsorption sites of Cu and NH_2 in the materials are more sensitive to water, and (3) the low water stability of MOF-199. The team of Xuejiao Sun [40] modified HKUST-1 with trivalent iron to obtain Fe-HK-2 with S_{BET} = 1400 and 1707 m^2/g and pore volume = 0.56 and 0.93 cm^3/g, respectively. The maximum adsorption of benzene by HKUST-1 was 11.4 mmol/g, and the maximum adsorption by Fe-HK-2 was 11.4 mmol/g, which was 1.5 times higher than before the modification. Barbara Szczęśniak's team [86] made composites of graphene (S_{BET} = 640 m^2/g, pore volume = 3.03 cm^3/g) and MOFs (S_{BET} = 3160 m^2/g, pore volume = 1.34 cm^3/g) in the ratios of (2:1, 1:1, 1:2) with S_{BET} = 990, 1510, and 2390 m^2/g and pore volume = 1.85, 1.62, and 1.76 cm^3/g. Among them, MG/MOF-1:2, which had the largest adsorption capacity for benzene, was 24.5 mmol/g at 20 °C, which was twice as much as the adsorption capacity of the MOFs. Although smaller than that of pure graphene, which is 33.6 mmol/g, it avoids the dilemma of the smaller adsorption capacity of graphene in medium–low relative pressure. Zhenxia Zhao's team [41] investigated the competitive adsorption of

benzene and water vapor on HKUST-1 (S_{BET} = 1568.5 m^2/g and pore volume = 0.75 cm^3/g), and they found that the material was more likely to form hydrogen bonds with water at low temperatures, thus inhibiting benzene adsorption. Furthermore, as the temperature increased, the material became more hydrophobic and more likely to adsorb benzene molecules. The system is shown in Figure 7a,b.

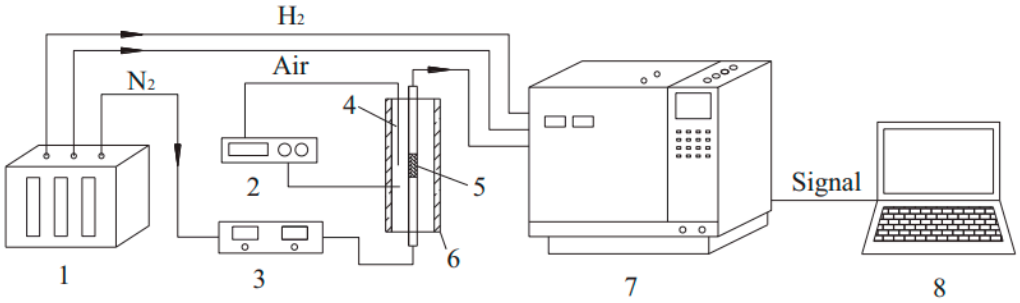

(1) gas generator; (2) temperature controller; (3) mass flow controller; (4) thermocouple; (5) stainless-steel column; (6) column furnace; (7) GC; (8) computer.

(**a**)

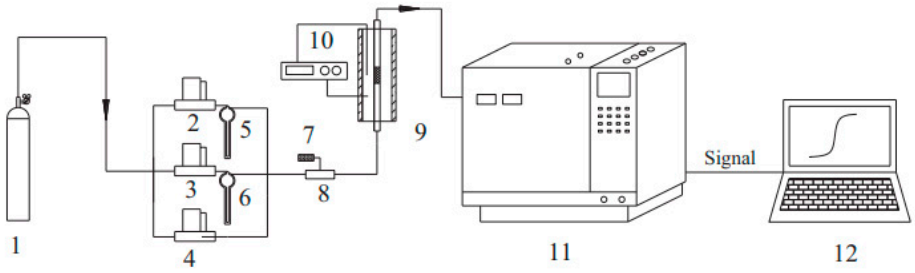

(1) N_2; (2,3,4) mass flow meter; (5) solvent saturator; (6) water saturator; (7) hygrometer; (8) gas mixing chamber; (9) adsorption chamber; (10) temperature controller; (11) GC; (12) computer.

(**b**)

Figure 7. (**a**) The experimental system for temperature-programmed desorption [41]. (**b**) Breakthrough experiment of benzene and water vapor [41].

3.1.4. Acetone Adsorption

Kun Yang's team [42] synthesized MOF-177 with S_{BET} = 2970 m^2/g and pore volume = 1.11 cm^3/g using the hydrothermal method, and the maximum adsorption capacity of 589 mg/g was obtained using adsorption experiments on acetone with 99.5% purity (Figure 8). By comparing the adsorption conclusions of the materials with other VOCs, it was found that although the particle size of acetone molecules is smaller than most of the BTEX molecules, their adsorption was lower than that of BTEX, which may be attributed to the fact that: (1) acetone molecules are more polar, (2) the acetone molecules were inaccessible due to a portion of the larger-sized microscopic pores possessed by the MOF-177, and (3) the BTEX molecules could form stronger interactions with the material compared with the acetone. This experiment supports the team's previous conclusion from studying MIL-101 for the adsorption of VOCs: when studying the adsorption of VOCs by MOFs, attention should be paid to the pore size and shape of the adsorbent and the molecular particle size of the adsorbent [87]. Yongbiao Wu's team [88] studied the adsorption process of acetone on MOF-5 using density functional theory and concluded that the large-cell cavity metal nest Zn_4O is the best adsorption site for acetone. Thus, it was proposed that more oxygen-containing functional groups could be introduced at the metal nest Zn_4O during the preparation of MOF-5 to enhance the adsorption effect

on acetone. Xin Zhou's team [89] used graphene oxide with the hydrothermal method with MIL-101 (S_{BET} = 2651 m^2/g, pore volume = 1.29 cm^3/g) to synthesize GrO@MIL-101 (S_{BET} = 2928 m^2/g, pore volume = 1.43 cm^3/g) to improve the adsorption of acetone. The adsorption capacity was enhanced from 13.92 mmol/g to 20.10 mmol/g at 288k, 161.6 mbar, an increase of 44%, and the cyclic adsorption capacity of the materials for acetone was enhanced. Denghui Li [90] team prepared MIL-101/TC with different contents of tobacco stem porous carbon mixed with MIL-101 (S_{BET} = 3974 m^2/g, average pore width = 2.26 nm, pore volume = 2.30 cm^3/g), in which there was a 10–20% decrease in BET surface area and total pore volume, an average pore width of around 20%, and up to a 19% increase in maximum adsorption capacity compared with the raw materials under ambient conditions.

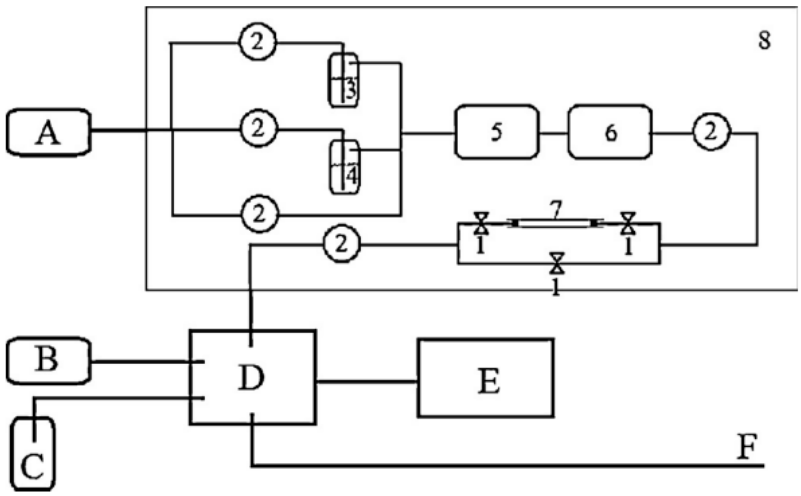

Figure 8. The dynamic adsorption equipment. A: air producer; B: H_2 producer; C: N_2 storage; D: GC; E: PC; and F: exhaust gas emission. (1): Valve; (2): mass flow meter; (3): liquid VOCs; (4): water; (5): mixing chamber; (6): stable chamber; (7): adsorption tube with MOF-177; (8): chamber with temperature control [42].

3.1.5. Xylene Adsorption

The MIL-101 synthesized by Zhenxia Zhao's team [91] adsorbed up to 10.9 mmol/g of xylene at 288 k and 6 bar, and 12.01, 9.67, 9.31, and 8.98 mmol/g of xylene at 288 k, 298 k, 308 k, and 318 k, respectively, using the Langmuir–Freundlich model. The heat of adsorption of xylene on the adsorbent was 24.8–44.3 kJ/mol. Patrick S's team [92] used synthesized UIO-66 (S_{BET} = 1050 m^2/g) to study the selectivity of xylene isomer adsorption. The results showed that the relatively larger volume of o-xylene was better adsorbed by the material, which may be due to the rotational freedom of the molecules within the cavity of the material. Jason A. Gee's team computer-screened xylene-sensitive materials and verified the conclusions with a breakthrough curve. The experimental conclusions were obtained with adsorption amounts of MIL-47, MIL-125-NH_2, MIL-140B, and MOF-48 at 5.7, 1.9, 1.7, and 2.6 mmol/cm^3, respectively [43].

3.1.6. Ethylbenzene Adsorption

Elnaz Jangodaz synthesized MIL-101(Cr) (S_{BET} = 2052.1 m^2/g, pore volume = 0.94 cm^3/g) and MIL-53(Fe) (S_{BET} = 1170.72 m^2/g, pore volume = 1.34 cm^3/g) in his laboratory to study the adsorption capacity of ethylbenzene at room temperature. At a concentration of 500 ppm, the two materials adsorbed 182, and 52 mg/g, respectively. From the analysis, the adsorption capacity of MIL-101(Cr) for ethylbenzene was not only due to its specific surface area and pore volume but also due to the formation of π-bond with ethylbenzene. The adsorption system is shown in Figure 9 [93]. In the MOF-177 and MIL-101 experiments of Kun Yang's team, the adsorption of ethylbenzene at room temperature was 234 and 1105 mg/g, respectively [42,87].

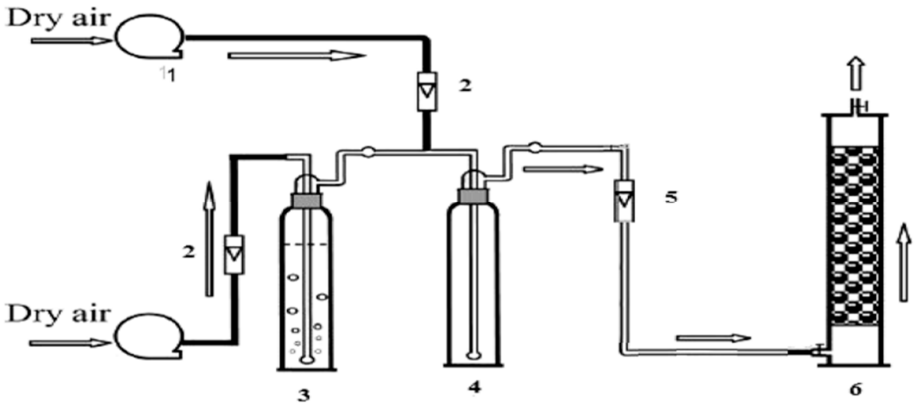

Figure 9. Adsorption apparatus system: (1) dry air; (2, 5) flowmeter; (3) BTEX column bubblizer; (4) mixed tank; and (6) adsorption column [93].

3.1.7. Dichloroethane Adsorption

Shikai Xian's team synthesized MIL-101(Cr) using microwave-assisted means. The maximum adsorption of 1,2-dichloroethane was measured to be 19 mmol/g at 288 k and 8 mbar, and the desorption effect reached up to 98.42% (Figure 10) [94]. Because the activation energy of water vapor on MIL-101(Cr) is greater than that of 1,2-dichloroethane, adsorption was affected by humid environments. The adsorption of 1,2-dichloroethane on MIL-101(Cr) at 5%, 40%, and 80% relative humidity under the condition of 303k was 2.282, 1.498, and 1.246 mmol/g respectively [95].

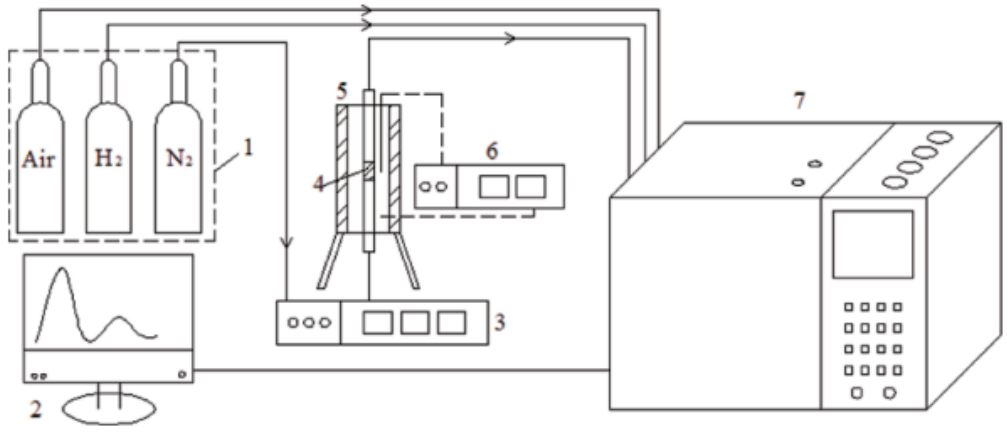

Figure 10. Adsorption system. (1) Feed gas; (2) display device; (3) mass flow controller; (4) stainless-steel column; (5) thermocouple; (6) temperature controller; and (7) gas chromatography [94].

3.2. Stability of the Adsorption Process

In order to ensure the reliability and safety of adsorption, it is necessary to ensure certain stability of the adsorption materials, including the stability of the materials itself water stability, thermal stability, etc.

3.2.1. Thermal Stability

The thermal degradation of MOFs is due to node–linker bond breakage accompanied by linker combustion, so the node–linker bond binding strength is highly correlated with the thermal stability of the materials [96]. Valentina Colombo's team [97] showed that three pyrazolyl ligands 1,3,5-tris(1H-pyrazol-4-yl) benzene (H_3BTP) and DMF in the excess reaction of metal acetates form the synthesis of microporous pyrazole acids bridging metal–organic backbone materials of the type $M_3(BTP)_2$-x solvent (M = Ni, Cu, Zn, Co), where S_{BET} = 1650, 1860, 930, and 1027 m^2/g were measured, respectively. Due to the special

structure of their synthesis, the materials obtained good thermal stability, where the Zn-containing materials could remain stable in air at 430 °C, even exceeding the thermal stability of zeolites. Colm Healy's team [98] found several empirical rules for improving thermal stability by studying and summarizing the results of others: (1) no solvents with inorganic nodes and chains, (2) the replacement of nodal entities with inorganic chains or sheets, (3) the use of relatively "hard" metal ions, and (4) no use of metal-bound functional groups. Joong Kang's team [99] compared the stability of several materials with uncoordinated organic bonds removed including MIL-53-Al, MIL-53-Cr, and MIL-47-V, and concluded that the thermal stability was MIL-53-Al > MIL-53-Cr > MIL-47-V. The reason was hypothesized experimentally to be that thermal stability is related to the strength of the metal–oxygen bonds. Shengqian Ma's team [100] synthesized a novel three-dimensional microporous metal–organic framework (PCN-17) of square planar Yb_4, which was extremely thermally stable due to its unique coordinately linked framework.

3.2.2. Chemical Stability

The chemical stability of MOFs is mainly in acid, alkali, and humid environments.

In general, the easiest way to determine the water stability of materials using an experiment is to expose them to a certain concentration of water vapor and then compare the exposed materials to the original material using an X-ray diffraction pattern. This method was used to determine whether a structure was disrupted [101]. Sebastian Zuluaga's team [102] found that the MOF-74 crystal structure was disrupted in a wet environment because the material dissociates H_2O, and the OH and H produced disintegrate the material. Therefore, they proposed modifying the material with metal ions, such as Zn, to inhibit the reaction. Cu-BTC(HKUST-1) is an excellent VOCs adsorption material at room temperature and pressure, and Yujie Li's team [103] designed a solvent-free mechanochemical method that quickly synthesized composites with different ratios of Cu-BTC and graphite oxide, and the maximum specific surface area of the modified material was 1362.7 m^2/g and the total pore volume was 0.87 cm^3/g. The maximum toluene uptake at 298 K was 9.1 mmol/g, which was 47% higher than that of the raw materials. More critically, the water stability of the material was greatly improved, the structure and pores were kept unchanged during water immersion, and the decrease in specific surface area was increased from the original 98.2% to 11.5%. Qingyuan Yang's team [104] prepared Zr-based MOFs with two carboxyl functional groups attached to the organism and verified its water vapor adsorption isotherm at 303 k with stability, and no collapse phenomenon was observed in PXRD patterns.

Tao He's team summarized several means to improve the chemical stability of materials: (1) combining high-valent metals with carboxylate ligands; (2) combining low-valent metals with azolate ligands; (3) improving the connectivity of building blocks; (4) making ligands tougher; (5) reinforcing the hydrophobicity of materials; and (6) replacing stabilized monoliths with stabilized monomer structures [105]. Keke Wang's team used trifluoromethyl as an insertion group to modify UiO-66 to improve the chemical stability of the material. The integrity of the material was maintained after washing with strong acids and bases [106]. In addition to strategies during synthesis, post-synthesis modifications likewise enhanced the chemical stability of the material. Tian-Fu Liu decomposed and oxidized the prepared PCN-426-Mg into two metal nodes to make the material more robust and stable [107].

3.3. Summary

The basic physical parameters and adsorption capacity of adsorbents are important features of the materials. The adsorption effect of the queried adsorbent materials on specific adsorbents reviewed in this section and the various attempts by researchers to enhance their adsorption performance are reviewed are summarized in Table 5. In addition, the stability of the materials is important for performance in the application of adsorbents to ensure that the materials do not collapse and crack during the adsorption process due to environmental conditions.

Table 5. Adsorption performance of MOFs.

MOFs	VOCs	Adsorption Method	Capacity	Reference
MIL-100(Fe)	toluene	static adsorption of pure steam	663 mg/g	[34]
MIL-101(Fe)	toluene	static adsorption of pure steam	180 mg/g	[34]
MIL-53(Fe)	toluene	static adsorption of pure steam	114 mg/g	[34]
UiO-66-NH_2	toluene	dynamic adsorption, penetration method (1000 ppm)	162 mg/g	[35]
MC-500-6	benzene	pure vapor	12.8 mmol/g	[85]
MOF-199	benzene	pure steam	6.4 mmol/g	[39]
Fe-HK-2	benzene	pure steam	11.4 mmol/g	[40]
MG/MOF-1:2	benzene	pure steam	24.5 mmol/g	[86]
MOF-177	acetone	pure steam	589 mg/g	[42]
GrO@MIL-101	acetone	pure steam	20.1 mmol/g	[89]
MIL-101	xylene	pure steam	10.9 mmol/g	[91]
MIL-101(Cr)	ethylbenzene	500ppm	182 mg/g	[93]
MIL-53(Fe)	ethylbenzene	550ppm	52 mg/g	[93]
MIL-101(Cr)	dichloroethane	-	19 mmol/g	[94]

4. MOF Applications

To benefit from the adsorption performance of MOFs toward VOCs and hazardous gas, researchers have explored specific application scenarios. In addition to their conventional use as adsorbents, many scholars have taken advantage of the high sensitivity of MOFs to VOCs and applied MOFs as probes on sensors to detect indoor VOCs concentrations. In laboratory settings, gas chromatography (GC) coupled with flame ionization detection (FID) or GC with electron capture detection (MS) analysis are the predominant methods for VOCs concentration detection. However, these instruments are often bulky with complex operations, lengthy analysis times, and high costs. While photoionization detectors (PIDs) and metal oxide-based chemical resistance sensors (MO) offer good VOCs response, they suffer limitations in multicomponent selectivity and are susceptible to interference from other substances [108]. Consequently, integrating MOFs into existing VOCs detection instruments holds significant promise, as it not only offers potential cost and energy savings but also enhances detection accuracy. According to previous studies in the literature [96–107], the chemical properties of the material and the chemical characteristics of the working environment have an important influence on air purification performance. For example, humid or watery environments require sufficient hydrophobicity of the material to avoid material destruction or water molecules occupying the adsorption sites; the thermo-chemical properties of the material should be evaluated for the application environment to avoid cracking of the material; and the chemical properties of the material should be modified for acid and alkali resistance when there are acid or alkaline gases in the environment. Therefore, before the actual application process, we should increase the research on the chemical properties of the environment and modify the properties of the materials according to the application scenarios so that the air purification performance of the materials can be better utilized.

Ye Bian's team [109] combined ZIF-67 with nanofibers to make filters and achieved 84% formaldehyde removal efficiency and efficient PM2.5 removal with good wind resistance. Wenhui Li's team [110] used MOF-derived ZnO to make hierarchical hollow nanocages as chemical sensing devices to detect ppm-level benzene and ppb-level acetone. S. Homayoonnia's team [111] synthesized CuBTC nanoparticles using an acoustic-chemical manner and coated them on a copper plate as a dielectric layer. Their results showed that the synthesized sensors could detect VOCs in a conventional environment (25 °C, RH10%). Yanlin Zhang's team [112] prepared Ni/Fe bimetallic MOFs using the hydrother-

mal method and changed the morphology of the materials using heat treatment with air at 350 °C to obtain $NiFe_2O_4$. The new materials were used to make VOCs sensors, and the experimental results revealed that the materials had a strong sensitivity to xylene in the detection of eight types of VOCs at 500 ppm. During the test for xylene alone, a good response was found from 10 to 1000 ppm transformed concentration. Christos Sapsanis's team [113] coated a capacitive sensor film with Cu(bdc)-xH_2O to detect the VOCs concentration. After water vapor tests, the detection results were found to be linear up to 65% relative humidity and nonlinear when the relative humidity was greater than 65% due to the interaction between metal spotting and hydrogen bonding adsorption. The detection results for acetone, ethanol, and methanol were found to be linear in the experiments for VOCs detection. The π-π bond generated on a benzene ring makes the film more sensitive to toluene, and the detection results were linear at low concentrations (125–500 ppm), but there will be errors. Di-Ming Chen's team [114] used 4,4′-oxy bis (benzoate) (H_2oba) to synthesize luminescent Tb-MOFs for the detection of VOCs vapor. During the experiment, a drop of the organic compound and a thin paper coated with the MOFs were placed into a colorimetric cup. The results were realistic because the materials completed the response to p-xylene vapor within 5 s with a 40% luminescence enhancement and stabilized within 5 min and the luminescence intensity of p-nitrobenzene decreased and reached half of the initial intensity within 3 min; although, the material responded weakly to other VOCs vapors. Tran Thanh Tung's team [115] used graphene to modify MOFs (pG-Cu BTC, pG-UiO 66, pG-ZIF 8) and fabricated chemo resistive sensors based on the materials for the detection of human-exhaled VOCs in order to provide early warning of certain diseases in humans. The experimental results showed that pG-Cu BTC had high sensitivity to chloroform and pG-UiO 66 had high sensitivity to methanol. Although the sensors for all three materials could measure the ppm concentration of VOCs, the intensity of the sensor response decreased with decreasing VOCs concentration (22.59–2.82 ppm). Huayun Chen's team [116] used a variety of flexible MOFs to fabricate VOCs sensors based on colorimetric mechanisms according to their breathing behavior. During the experiment, fresh tomato leaves and disease-causing spores were incubated together as a source of VOCs, and the sensors were used to detect VOCs to determine if the plant was healthy or not, and the results proved to be 96.7% accurate.

5. Summary and Potential

Presently, solid adsorption stands as a notably more enduring and secure approach for the regulation of indoor pollutants. The pivotal avenue for enhancing the efficacy of solid adsorption systems revolves around the acquisition of adsorbents characterized by pronounced water stability, thermal resilience, and a heightened adsorption capacity. In contrast to established adsorbent modalities, MOFs exhibit augmented specific surface areas and pore volumes. Furthermore, they manifest an intrinsically more suitable molecular architecture conducive to the adsorption of VOCs, coupled with a substantial capacity for tailored modification. This renders MOFs progressively poised to emerge as a prospective substitute for conventional adsorbents. A majority of documented MOFs adsorption trials are typified by ambient temperature and pressure conditions, thereby corroborating the suitability of these materials for human inhabitation contexts.

Among the synthesis methods for MOFs, the hydrothermal method remains the most important due to its simple operation and stability. With the introduction of auxiliary methods such as electrochemistry and microwave, the synthesis time has been shortened, the stability of materials has been enhanced, the amount of waste liquid has been reduced, and energy and raw material consumption have been reduced to a certain extent, making the synthesis process more environmentally friendly. To study the adsorption mechanism, due to the significant differences in the adsorption process between different adsorbents and volatile organic compounds, a large number of validation experiments need to be conducted. However, we can briefly summarize some conclusions: (1) An increase in metal sites can strengthen the adsorption of most VOCs molecules. (2) The formation of π-bonds

can enhance the adsorption of molecules containing benzene ring VOCs. (3) The effect of hydrogen bonds is relatively weak in the adsorption mechanism, but the presence of H-atoms can strengthen the adsorption of VOCs such as toluene. (4) The enhancement of electrostatic forces strengthens the adsorption of polar VOCs molecules. Previous studies on the adsorption performance of VOCs have focused on the adsorption of single VOCs, and a great deal of research is still needed on the adsorption performance of multi-component VOCs adsorption and the adsorption performance of air-contained VOCs in real-life situations, especially on whether the competitive adsorption of multi-component VOCs affects the overall adsorption effect. Using single VOCs adsorption experiments, it was demonstrated that an increase in temperature decreases the adsorption capacity of MOFs, and an increase in relative humidity also decreases the adsorption capacity of MOFs. However, these experiments were based on high concentrations of VOCs, and experiments on low concentrations of VOCs (ppb level) are missing.

With continuous exploration by scientists, the synthesis and performance of MOFs have been significantly advanced. The modification of materials can increase their stability and adsorption capacity and resist the interference of the external environment. However, of the materials reported in the last 20 years, from synthesis to application, none are perfect in every way and are not as stable and mass-produced as something like silica gel. Based on the reviewed information, we summarize some suggestions for the future direction of materials research:

(1) Considering the safety of the habitat environment, reduce the introduction of heavy metal ions and toxic substances in the synthesis to ensure the safety of the synthesis and use stages.
(2) During the performance analysis of materials, pay attention to cyclic adsorption experiments to verify whether the adsorption performance of the materials decreases or if the materials crack during the cyclic process.
(3) For MOFs applied in the habitat environment, using ppb-level VOCs as adsorbents, determine whether the adsorption law at low concentration is equivalent to that at a high concentration of VOCs and whether the adsorption mechanism will change.
(4) Adsorption experiments in an actual room environment will be a very interesting topic, not to create specific components of VOCs, but to use paints, plywood, and other actual decoration materials as the source of VOCs.
(5) For a solid rotary wheel, determine how to really eliminate the VOCs adsorbed by the materials rather than just blowing them out. This will greatly increase the use scenario of wheels. We do not do pollutants mover, we do pollutants cleaner.

Author Contributions: Writing—review and editing, K.W.; methodology and idea proposal, J.N.; validation and formal analysis, H.H.; visualization, F.H.; project administration and funding acquisition, J.N. All authors have read and agreed to the published version of the manuscript.

Funding: This work was supported by the National Key R&D Program of China (NO. 2021YFF0306305), the National Natural Science Foundation of China (No. 51708013), and the Pyramid talent training project of the Beijing University of Civil Engineering and Architecture (No. JDJQ20200303).

Institutional Review Board Statement: Not applicable. This article does not involve experiments on humans or animals.

Informed Consent Statement: Not applicable. This article does not deal with experiments on humans.

Data Availability Statement: Not applicable. This paper does not involve specific experimental parameters.

Conflicts of Interest: The authors declare no conflict of interest.

References

1. Wei, Y. Emission Strength Estimates and Source Apportionment of VOCs in Winter Residential Indoor Environment. Master's Thesis, Chang'an University, Xi'an, China, 2002.
2. Klepeis, N.E.; Nelson, W.C.; Ott, W.R.; Robinson, J.P.; Tsang, A.M.; Switzer, P.; Behar, J.V.; Hern, S.C.; Engelmann, W.H. The National Human Activity Pattern Survey (NHAPS): A resource for assessing exposure to environmental pollutants. *J. Expo. Sci. Environ. Epidemiol.* **2001**, *11*, 231–252. [CrossRef] [PubMed]
3. Adgate, J.L.; Church, T.R.; Ryan, A.D.; Ramachandran, G.; Fredrickson, A.L.; Stock, T.H.; Morandi, M.T.; Sexton, K. Outdoor, Indoor, and Personal Exposure to VOCs in Children. *Environ. Health Perspect.* **2004**, *112*, 1386–1392. [CrossRef] [PubMed]
4. Jia, C.; Cao, K.; Valaulikar, R.; Fu, X.; Sorin, A.B. Variability of Total Volatile Organic Compounds (TVOC) in the Indoor Air of Retail Stores. *Int. J. Environ. Res. Public Health* **2019**, *16*, 4622. [CrossRef] [PubMed]
5. Zhang, J.F.; Smith, K.R. Indoor air pollution: A global health concern. *Br. Med. Bull.* **2003**, *68*, 209–225. [CrossRef]
6. World Health Organization. Indoor air quality: Organic pollutants. *Environ. Technol. Lett.* **1989**, *10*, 855–858. [CrossRef]
7. Portela, N.B.; Teixeira, E.C.; Agudelo-Castañeda, D.M.; Civeira, M.d.S.; Silva, L.F.O.; Vigo, A.; Kumar, P. Indoor-outdoor relationships of airborne nanoparticles, BC and VOCs at rural and urban preschools. *Environ. Pollut.* **2020**, *268*, 115751. [CrossRef]
8. Arı, A.; Arı, P.E.; Yenisoy-Karakaş, S.; Gaga, E.O. Source characterization and risk assessment of occupational exposure to volatile organic compounds (VOCs) in a barbecue restaurant. *Build. Environ.* **2020**, *174*, 106791. [CrossRef]
9. Boyle, E.B.; Viet, S.M.; Wright, D.J.; Merrill, L.S.; Alwis, K.U.; Blount, B.C.; Mortensen, M.E.; Moye, J., Jr.; Dellarco, M. Assessment of Exposure to VOCs among Pregnant Women in the National Children's Study. *Int. J. Environ. Res. Public Health* **2016**, *13*, 376. [CrossRef]
10. Tagiyeva, N.; Sheikh, A. Domestic exposure to volatile organic compounds in relation to asthma and allergy in children and adults. *Expert Rev. Clin. Immunol.* **2014**, *10*, 1611–1639. [CrossRef]
11. Rahman, M.; Kim, K.-H. Exposure to hazardous volatile pollutants back diffusing from automobile exhaust systems. *J. Hazard. Mater.* **2012**, *241–242*, 267–278. [CrossRef]
12. He, Z.; Li, G.; Chen, J.; Huang, Y.; An, T.; Zhang, C. Pollution characteristics and health risk assessment of volatile organic compounds emitted from different plastic solid waste recycling workshops. *Environ. Int.* **2015**, *77*, 85–94. [CrossRef] [PubMed]
13. Shen, J.; Liu, Y.; Zhang, X.-W.; Liu, M. Study on the Volatile Compounds Emission from Wood-based Composites. *China For. Prod. Ind.* **2006**, *1*, 5–9.
14. Zhao, Q.; Li, Y.; Chai, X.; Xu, L.; Zhang, L.; Ning, P.; Huang, J.; Tian, S. Interaction of inhalable volatile organic compounds and pulmonary surfactant: Potential hazards of VOCs exposure to lung. *J. Hazard. Mater.* **2019**, *369*, 512–520. [CrossRef]
15. Bentayeb, M.; Billionnet, C.; Baiz, N.; Derbez, M.; Kirchner, S.; Annesi-Maesano, I. Higher prevalence of breathlessness in elderly exposed to indoor aldehydes and VOCs in a representative sample of French dwellings. *Respir. Med.* **2013**, *107*, 1598–1607. [CrossRef] [PubMed]
16. Billionnet, C.; Gay, E.; Kirchner, S.; Leynaert, B.; Annesi-Maesano, I. Quantitative assessments of indoor air pollution and respiratory health in a population-based sample of French dwellings. *Environ. Res.* **2011**, *111*, 425–434. [CrossRef] [PubMed]
17. Wang, X.; Chuai, Y.; Wang, L.; Jan, S. Association between and indoor VOCs and asthma, allergic rhinitis, eczema in preschool children. *Environ. Chem.* **2018**, *37*, 1901–1909.
18. Berenjian, A.; Chan, N.; Malmiri, H.J. Volatile Organic Compounds Removal Methods: A Review. *Am. J. Biochem. Biotechnol.* **2012**, *8*, 220–229. [CrossRef]
19. Zhang, Z.; Jiang, Z.; Shangguan, W. Low-temperature catalysis for VOCs removal in technology and application: A state-of-the-art review. *Catal. Today* **2016**, *264*, 270–278. [CrossRef]
20. Chung, W.-C.; Mei, D.-H.; Tu, X.; Chang, M.-B. Removal of VOCs from gas streams via plasma and catalysis. *Catal. Rev.* **2018**, *61*, 270–331. [CrossRef]
21. Meng, G. Study on Response of Several Indoor Plants to The Compound Pollution of Benzene and Formaldehyde. Ph.D. Thesis, Nanjing Forestry University, Nanjing, China, 2013.
22. Lu, Y.; Liu, J.; Lu, B.; Jiang, A.; Wan, C. Study on the removal of indoor VOCs using biotechnology. *J. Hazard. Mater.* **2010**, *182*, 204–209. [CrossRef]
23. Hamad, A.; Fayed, M. Simulation-Aided Optimization of Volatile Organic Compounds Recovery Using Condensation. *Chem. Eng. Res. Des.* **2004**, *82*, 895–906. [CrossRef]
24. Parthasarathy, G.; El-Halwagi, M.M. Optimum mass integration strategies for condensation and allocation of multicomponent VOCs. *Chem. Eng. Sci.* **2000**, *55*, 881–895. [CrossRef]
25. Davis, R.J.; Zeiss, R.F. Cryogenic condensation: A cost-effective technology for controlling VOC emissions. *Environ. Prog.* **2002**, *21*, 111–115. [CrossRef]
26. Gan, G.; Fan, S.; Li, X.; Zhang, Z.; Hao, Z. Adsorption and membrane separation for removal and recovery of volatile organic compounds. *J. Environ. Sci.* **2023**, *123*, 96–115. [CrossRef]
27. Yang, C.; Miao, G.; Pi, Y.; Xia, Q.; Wu, J.; Li, Z.; Xiao, J. Abatement of various types of VOCs by adsorption/catalytic oxidation: A review. *Chem. Eng. J.* **2019**, *370*, 1128–1153. [CrossRef]
28. Xiang, W.; Zhang, X.; Chen, K.; Fang, J.; He, F.; Hu, X.; Tsang, D.C.; Ok, Y.S.; Gao, B. Enhanced adsorption performance and governing mechanisms of ball-milled biochar for the removal of volatile organic compounds (VOCs). *Chem. Eng. J.* **2019**, *385*, 123842. [CrossRef]

29. Vellingiri, K.; Kumar, P.; Deep, A.; Kim, K.H. Metal-organic frameworks for the adsorption of gaseous toluene under ambient temperature and pressure. *Chem. Eng. J.* **2017**, *307*, 1116–1126. [CrossRef]
30. Li, X.; Zhang, L.; Yang, Z.; Wang, P.; Yan, Y.; Ran, J. Adsorption materials for volatile organic compounds (VOCs) and the key factors for VOCs adsorption process: A review. *Sep. Purif. Technol.* **2019**, *235*, 116213. [CrossRef]
31. Wu, X.; Bao, Z.; Yuan, B.; Wang, J.; Sun, Y.; Luo, H.; Deng, S. Microwave synthesis and characterization of MOF-74 (M = Ni, Mg) for gas separation. *Microporous Mesoporous Mater.* **2013**, *180*, 114–122. [CrossRef]
32. Haque, E.; Jhung, S.H. Synthesis of isostructural metal–organic frameworks, CPO-27s, with ultrasound, microwave, and conventional heating: Effect of synthesis methods and metal ions. *Chem. Eng. J.* **2011**, *173*, 866–872. [CrossRef]
33. Wang, D.; Wu, G.; Zhao, Y.; Cui, L.; Shin, C.-H.; Ryu, M.-H.; Cai, J. Study on the copper(II)-doped MIL-101(Cr) and its performance in VOCs adsorption. *Environ. Sci. Pollut. Res.* **2018**, *25*, 28109–28119. [CrossRef]
34. Ma, X.; Wang, W.; Sun, C.; Li, H.; Sun, J.; Liu, X. Adsorption performance and kinetic study of hierarchical porous Fe-based MOFs for toluene removal. *Sci. Total. Environ.* **2021**, *793*, 148622. [CrossRef]
35. Shi, X.; Zhang, X.; Bi, F.; Zheng, Z.; Sheng, L.; Xu, J.; Wang, Z.; Yang, Y. Effective toluene adsorption over defective UiO-66-NH_2: An experimental and computational exploration. *J. Mol. Liq.* **2020**, *316*, 113812. [CrossRef]
36. Vo, T.K.; Le, V.N.; Nguyen, V.C.; Song, M.; Kim, D.; Yoo, K.S.; Park, B.J.; Kim, J. Microwave-assisted continuous-flow synthesis of mixed-ligand UiO-66(Zr) frameworks and their application to toluene adsorption. *J. Ind. Eng. Chem.* **2020**, *86*, 178–185. [CrossRef]
37. Bellat, J.-P.; Bezverkhyy, I.; Weber, G.; Royer, S.; Averlant, R.; Giraudon, J.-M.; Lamonier, J.-F. Capture of formaldehyde by adsorption on nanoporous materials. *J. Hazard. Mater.* **2015**, *300*, 711–717. [CrossRef]
38. Wang, Z.; Wang, W.; Jiang, D.; Zhang, L.; Zheng, Y. Diamine-appended metal–organic frameworks: Enhanced formaldehyde-vapor adsorption capacity, superior recyclability and water resistibility. *Dalton Trans.* **2016**, *45*, 11306–11311. [CrossRef]
39. Liu, B.; Younis, S.A.; Kim, K.-H. The dynamic competition in adsorption between gaseous benzene and moisture on metal-organic frameworks across their varying concentration levels. *Chem. Eng. J.* **2020**, *421*, 127813. [CrossRef]
40. Sun, X.; Gu, X.; Xu, W.; Chen, W.-J.; Xia, Q.; Pan, X.; Zhao, X.; Li, Y.; Wu, Q.-H. Novel Hierarchical Fe(III)-Doped Cu-MOFs With Enhanced Adsorption of Benzene Vapor. *Front. Chem.* **2019**, *7*, 652. [CrossRef] [PubMed]
41. Zhao, Z.; Wang, S.; Yang, Y.; Li, X.; Li, J.; Li, Z. Competitive adsorption and selectivity of benzene and water vapor on the microporous metal organic frameworks (HKUST-1). *Chem. Eng. J.* **2015**, *259*, 79–89. [CrossRef]
42. Yang, K.; Xue, F.; Sun, Q.; Yue, R.; Lin, D. Adsorption of volatile organic compounds by metal-organic frameworks MOF-177. *J. Environ. Chem. Eng.* **2013**, *1*, 713–718. [CrossRef]
43. Gee, J.A.; Zhang, K.; Bhattacharyya, S.; Bentley, J.; Rungta, M.; Abichandani, J.S.; Sholl, D.S.; Nair, S. Computational Identification and Experimental Evaluation of Metal–Organic Frameworks for Xylene Enrichment. *J. Phys. Chem. C* **2016**, *120*, 12075–12082. [CrossRef]
44. Sui, H.; Wang, Z.; He, L.; Han, Z.; Li, X. Piecewise loading bed for reversible adsorption of VOCs on silica gels. *J. Taiwan Inst. Chem. Eng.* **2019**, *102*, 51–60. [CrossRef]
45. Sui, H.; An, P.; Li, X.; Cong, S.; He, L. Removal and recovery of *o*-xylene by silica gel using vacuum swing adsorption. *Chem. Eng. J.* **2017**, *316*, 232–242. [CrossRef]
46. Kim, K.-J.; Ahn, H.-G. The effect of pore structure of zeolite on the adsorption of VOCs and their desorption properties by microwave heating. *Microporous Mesoporous Mater.* **2012**, *152*, 78–83. [CrossRef]
47. Lee, D.-G.; Kim, J.-H.; Lee, C.-H. Adsorption and thermal regeneration of acetone and toluene vapors in dealuminated Y-zeolite bed. *Sep. Purif. Technol.* **2011**, *77*, 312–324. [CrossRef]
48. Baytar, O.; Şahin, ö.; Horoz, S.; Kutluay, S. High-performance gas-phase adsorption of benzene and toluene on activated carbon: Response surface optimization, reusability, equilibrium, kinetic, and competitive adsorption studies. *Environ. Sci. Pollut. Res.* **2020**, *27*, 26191–26210. [CrossRef] [PubMed]
49. Carvajal-Bernal, A.M.; Gómez-Granados, F.; Giraldo, L.; Moreno-Piraján, J.C. Influence of stacked structure of carbons modified on its surface on n-pentane adsorption. *Heliyon* **2019**, *5*, e01156. [CrossRef]
50. Stock, N.; Biswas, S. Synthesis of Metal-Organic Frameworks (MOFs): Routes to Various MOF Topologies, Morphologies, and Composites. *Chem. Rev.* **2011**, *112*, 933–969. [CrossRef]
51. Rubio-Martinez, M.; Avci-Camur, C.; Thornton, A.W.; Imaz, I.; Maspoch, D.; Hill, M.R. New synthetic routes towards MOF production at scale. *Chem. Soc. Rev.* **2017**, *46*, 3453–3480. [CrossRef]
52. McKinstry, C.; Cathcart, R.J.; Cussen, E.J.; Fletcher, A.J.; Patwardhan, S.V.; Sefcik, J. Scalable continuous solvothermal synthesis of metal organic framework (MOF-5) crystals. *Chem. Eng. J.* **2016**, *285*, 718–725. [CrossRef]
53. Feng, D.; Wang, K.; Wei, Z.; Chen, Y.-P.; Simon, C.M.; Arvapally, R.K.; Martin, R.L.; Bosch, M.; Liu, T.-F.; Fordham, S.; et al. Kinetically tuned dimensional augmentation as a versatile synthetic route towards robust metal–organic frameworks. *Nat. Commun.* **2014**, *5*, 5723. [CrossRef] [PubMed]
54. Millange, F.; El Osta, R.; Medina, M.E.; Walton, R.I. A time-resolved diffraction study of a window of stability in the synthesis of a copper carboxylate metal–organic framework. *CrystEngComm* **2010**, *13*, 103–108. [CrossRef]
55. Biemmi, E.; Christian, S.; Stock, N.; Bein, T. High-throughput screening of synthesis parameters in the formation of the metal-organic frameworks MOF-5 and HKUST-1. *Microporous Mesoporous Mater.* **2009**, *117*, 111–117. [CrossRef]
56. Thomas-Hillman, I.; Laybourn, A.; Dodds, C.; Kingman, S.W. Realising the environmental benefits of metal–organic frameworks: Recent advances in microwave synthesis. *J. Mater. Chem. A* **2018**, *6*, 11564–11581. [CrossRef]

57. Vakili, R.; Xu, S.; Al-Janabi, N.; Gorgojo, P.; Holmes, S.M.; Fan, X. Microwave-assisted synthesis of zirconium-based metal organic frameworks (MOFs): Optimization and gas adsorption. *Microporous Mesoporous Mater.* **2018**, *260*, 45–53. [CrossRef]
58. Khan, N.A.; Jhung, S.H. Synthesis of metal-organic frameworks (MOFs) with microwave or ultrasound: Rapid reaction, phase-selectivity, and size reduction. *Coord. Chem. Rev.* **2015**, *285*, 11–23. [CrossRef]
59. Haque, E.; Khan, N.A.; Park, J.H.; Jhung, S.H. Synthesis of a Metal-Organic Framework Material, Iron Terephthalate, by Ultrasound, Microwave, and Conventional Electric Heating: A Kinetic Study. *Chem. A Eur. J.* **2009**, *16*, 1046–1052. [CrossRef]
60. Ameloot, R.; Stappers, L.; Fransaer, J.; Alaerts, L.; Sels, B.F.; De Vos, D.E. Patterned Growth of Metal-Organic Framework Coatings by Electrochemical Synthesis. *Chem. Mater.* **2009**, *21*, 2580–2582. [CrossRef]
61. Neto, O.J.d.L.; Frós, A.C.d.O.; Barros, B.S.; Monteiro, A.F.d.F.; Kulesza, J. Rapid and efficient electrochemical synthesis of a zinc-based nano-MOF for Ibuprofen adsorption. *New J. Chem.* **2019**, *43*, 5518–5524. [CrossRef]
62. Pirzadeh, K.; Ghoreyshi, A.A.; Rahimnejad, M.; Mohammadi, M. Electrochemical synthesis, characterization and application of a microstructure Cu3(BTC)2 metal organic framework for CO_2 and CH_4 separation. *Korean J. Chem. Eng.* **2018**, *35*, 974–983. [CrossRef]
63. Szczęśniak, B.; Borysiuk, S.; Choma, J.; Jaroniec, M. Mechanochemical synthesis of highly porous materials. *Mater. Horiz.* **2020**, *7*, 1457–1473. [CrossRef]
64. Lv, D.; Chen, Y.; Li, Y.; Shi, R.; Wu, H.; Sun, X.; Xiao, J.; Xi, H.; Xia, Q.; Li, Z. Efficient Mechanochemical Synthesis of MOF-5 for Linear Alkanes Adsorption. *J. Chem. Eng. Data* **2017**, *62*, 2030–2036. [CrossRef]
65. Chen, Y.; Wu, H.; Liu, Z.; Sun, X.; Xia, Q.; Li, Z. Liquid-assisted mechanochemical synthesis of copper based MOF-505 for the separation of CO_2 over CH_4 or N_2. *Ind. Eng. Chem. Res.* **2018**, *57*, 703–709. [CrossRef]
66. Khan, N.A.; Hasan, Z.; Jhung, S.H. Adsorptive removal of hazardous materials using metal-organic frameworks (MOFs): A review. *J. Hazard. Mater.* **2013**, *244–245*, 444–456. [CrossRef]
67. Huang, C.-Y.; Song, M.; Gu, Z.-Y.; Wang, H.-F.; Yan, X.-P. Probing the Adsorption Characteristic of Metal–Organic Framework MIL-101 for Volatile Organic Compounds by Quartz Crystal Microbalance. *Environ. Sci. Technol.* **2011**, *45*, 4490–4496. [CrossRef]
68. Vikrant, K.; Kim, K.-H.; Kumar, V.; Giannakoudakis, D.A.; Boukhvalov, D.W. Adsorptive removal of an eight-component volatile organic compound mixture by Cu-, Co-, and Zr-metal-organic frameworks: Experimental and theoretical studies. *Chem. Eng. J.* **2020**, *397*, 125391. [CrossRef]
69. Ma, F.-J.; Liu, S.-X.; Liang, D.-D.; Ren, G.-J.; Wei, F.; Chen, Y.-G.; Su, Z.-M. Adsorption of volatile organic compounds in porous metal–organic frameworks functionalized by polyoxometalates. *J. Solid State Chem.* **2011**, *184*, 3034–3039. [CrossRef]
70. Trens, P.; Belarbi, H.; Shepherd, C.; Gonzalez, P.; Ramsahye, N.A.; Lee, U.-H.; Seo, Y.-K.; Chang, J.-S. Coadsorption of *n*-Hexane and Benzene Vapors onto the Chromium Terephthalate-Based Porous Material MIL-101(Cr) An Experimental and Computational Study. *J. Phys. Chem. C* **2012**, *116*, 25824–25831. [CrossRef]
71. Vellingiri, K.; Szulejko, J.E.; Kumar, P.; Kwon, E.E.; Kim, K.-H.; Deep, A.; Boukhvalov, D.W.; Brown, R.J.C. Metal organic frameworks as sorption media for volatile and semi-volatile organic compounds at ambient conditions. *Sci. Rep.* **2016**, *6*, 27813. [CrossRef]
72. Duan, C.; Yu, Y.; Yang, P.; Zhang, X.; Li, F.; Li, L.; Xi, H. Engineering New Defects in MIL-100(Fe) via a Mixed-Ligand Approach To Effect Enhanced Volatile Organic Compound Adsorption Capacity. *Ind. Eng. Chem. Res.* **2019**, *59*, 774–782. [CrossRef]
73. Saini, V.K.; Pires, J. Development of metal organic framework-199 immobilized zeolite foam for adsorption of common indoor VOCs. *J. Environ. Sci.* **2017**, *55*, 321–330. [CrossRef] [PubMed]
74. Wang, L.; Liang, X.-Y.; Chang, Z.-Y.; Ding, L.-S.; Zhang, S.; Li, B.-J. Effective Formaldehyde Capture by Green Cyclodextrin-Based Metal–Organic Framework. *ACS Appl. Mater. Interfaces* **2017**, *10*, 42–46. [CrossRef]
75. Severino, M.I.; Al Mohtar, A.; Soares, C.V.; Freitas, C.; Sadovnik, N.; Nandi, S.; Mouchaham, G.; Pimenta, V.; Nouar, F.; Daturi, M.; et al. MOFs with Open Metal(III) Sites for the Environmental Capture of Polar Volatile Organic Compounds. *Angew. Chem. Int. Ed.* **2022**, *62*, e202211583. [CrossRef]
76. Luebbers, M.T.; Wu, T.; Shen, L.; Masel, R.I. Trends in the Adsorption of Volatile Organic Compounds in a Large-Pore Metal−Organic Framework, IRMOF-1. *Langmuir* **2010**, *26*, 11319–11329. [CrossRef] [PubMed]
77. Wu, Y.; Liu, D.; Wu, Y.; Qian, Y.; Xi, H. Effect of electrostatic properties of IRMOFs on VOCs adsorption: A density functional theory study. *Adsorption* **2014**, *20*, 777–788. [CrossRef]
78. Ahmad, A.; Ali, M.; Al-Sehemi, A.G.; Al-Ghamdi, A.A.; Park, J.-W.; Algarni, H.; Anwer, H. Carbon-integrated semiconductor photocatalysts for removal of volatile organic compounds in indoor environments. *Chem. Eng. J.* **2023**, *452*, 139436. [CrossRef]
79. Alhamami, M.; Doan, H.; Cheng, C.-H. A Review on Breathing Behaviors of Metal-Organic-Frameworks (MOFs) for Gas Adsorption. *Materials* **2014**, *7*, 3198–3250. [CrossRef]
80. Yaghi, O.M.; Li, G.; Li, H. Selective binding and removal of guests in a microporous metal–organic framework. *Nature* **1995**, *378*, 703–706. [CrossRef]
81. Yaghi, O.M.; Li, H. Hydrothermal Synthesis of a Metal-Organic Framework Containing Large Rectangular Channels. *J. Am. Chem. Soc.* **1995**, *117*, 10401–10402. [CrossRef]
82. Eddaoudi, M.; Kim, J.; Rosi, N.; Vodak, D.; Wachter, J.; O'Keeffe, M.; Yaghi, O.M. Systematic Design of Pore Size and Functionality in Isoreticular MOFs and Their Application in Methane Storage. *Science* **2002**, *295*, 469–472. [CrossRef]
83. Duan, C.; Yang, M.; Li, F.; Li, Y.; Peng, A.; Luo, S.; Xi, H. Soft-templating Synthesis of Mesoporous Metal–Organic Frameworks with Enhanced Toluene Adsorption Capacity. *ChemistrySelect* **2018**, *3*, 12888–12893. [CrossRef]

84. Xu, W.-Q.; He, S.; Lin, C.-C.; Qiu, Y.-X.; Liu, X.-J.; Jiang, T.; Liu, W.-T.; Zhang, X.-L.; Jiang, J.-J. A copper based metal-organic framework: Synthesis, modification and VOCs adsorption. *Inorg. Chem. Commun.* **2018**, *92*, 1–4. [CrossRef]
85. Wang, C.; Yin, H.; Tian, P.; Sun, X.; Pan, X.; Chen, K.; Chen, W.-J.; Wu, Q.-H.; Luo, S. Remarkable adsorption performance of MOF-199 derived porous carbons for benzene vapor. *Environ. Res.* **2020**, *184*, 109323. [CrossRef] [PubMed]
86. Szczęśniak, B.; Choma, J.; Jaroniec, M. Ultrahigh benzene adsorption capacity of graphene-MOF composite fabricated via MOF crystallization in 3D mesoporous graphene. *Microporous Mesoporous Mater.* **2019**, *279*, 387–394. [CrossRef]
87. Yang, K.; Sun, Q.; Xue, F.; Lin, D. Adsorption of volatile organic compounds by metal–organic frameworks MIL-101: Influence of molecular size and shape. *J. Hazard. Mater.* **2011**, *195*, 124–131. [CrossRef]
88. Wu, Y.; Liu, D.; Wu, Y.; Xi, H. Adsorption mechanism of methanol, acetaldehyde and acetone on MOF-5 with density functional theory. *CIESC J.* **2013**, *64*, 2891–2897.
89. Zhou, X.; Huang, W.; Shi, J.; Zhao, Z.; Xia, Q.; Li, Y.; Wang, H.; Li, Z. A novel MOF/graphene oxide composite GrO@ MIL-101 with high adsorption capacity for acetone. *J. Mater. Chem. A* **2014**, *2*, 4722–4730. [CrossRef]
90. Li, D.; Li, L.; Chen, R.; Wang, C.; Li, H.; Li, H. A MIL-101 Composite Doped with Porous Carbon from Tobacco Stem for Enhanced Acetone Uptake at Normal Temperature. *Ind. Eng. Chem. Res.* **2018**, *57*, 6226–6235. [CrossRef]
91. Zhao, Z.; Li, X.; Li, Z. Adsorption equilibrium and kinetics of p-xylene on chromium-based metal organic framework MIL-101. *Chem. Eng. J.* **2011**, *173*, 150–157. [CrossRef]
92. Bárcia, P.S.; Guimarães, D.; Mendes, P.A.; Silva, J.A.; Guillerm, V.; Chevreau, H.; Serre, C.; Rodrigues, A.E. Reverse shape selectivity in the adsorption of hexane and xylene isomers in MOF UiO-66. *Microporous Mesoporous Mater.* **2011**, *139*, 67–73. [CrossRef]
93. Jangodaz, E.; Alaie, E.; Safekordi, A.A.; Tasharrofi, S. Adsorption of Ethylbenzene from Air on Metal–Organic Frameworks MIL-101(Cr) and MIL-53(Fe) at Room Temperature. *J. Inorg. Organomet. Polym. Mater.* **2018**, *28*, 2090–2099. [CrossRef]
94. Xian, S.; Li, X.; Xu, F.; Xia, Q.; Li, Z. Adsorption Isotherms, Kinetics, and Desorption of 1,2-Dichloroethane on Chromium-Based Metal Organic Framework MIL-101. *Sep. Sci. Technol.* **2013**, *48*, 1479–1489. [CrossRef]
95. Xian, S.; Yu, Y.; Xiao, J.; Zhang, Z.; Xia, Q.; Wang, H.; Li, Z. Competitive adsorption of water vapor with VOCs dichloroethane, ethyl acetate and benzene on MIL-101(Cr) in humid atmosphere. *RSC Adv.* **2014**, *5*, 1827–1834. [CrossRef]
96. Bennett, T.D.; Goodwin, A.L.; Dove, M.T.; Keen, D.A.; Tucker, M.G.; Barney, E.R.; Soper, A.K.; Bithell, E.G.; Tan, J.-C.; Cheetham, A.K. Structure and Properties of an Amorphous Metal-Organic Framework. *Phys. Rev. Lett.* **2010**, *104*, 115503. [CrossRef]
97. Colombo, V.; Galli, S.; Choi, H.J.; Han, G.D.; Maspero, A.; Palmisano, G.; Masciocchi, N.; Long, J.R. High thermal and chemical stability in pyrazolate-bridged metal–organic frameworks with exposed metal sites. *Chem. Sci.* **2011**, *2*, 1311–1319. [CrossRef]
98. Healy, C.; Patil, K.M.; Wilson, B.H.; Hermanspahn, L.; Harvey-Reid, N.C.; Howard, B.I.; Kleinjan, C.; Kolien, J.; Payet, F.; Telfer, S.G.; et al. The thermal stability of metal-organic frameworks. *Coord. Chem. Rev.* **2020**, *419*, 213388. [CrossRef]
99. Kang, I.J.; Khan, N.A.; Haque, E.; Jhung, S.H. Chemical and Thermal Stability of Isotypic Metal–Organic Frameworks: Effect of Metal Ions. *Chem. A Eur. J.* **2011**, *17*, 6437–6442. [CrossRef]
100. Ma, S.; Wang, X.-S.; Yuan, D.; Zhou, H.-C. A Coordinatively Linked Yb Metal–Organic Framework Demonstrates High Thermal Stability and Uncommon Gas-Adsorption Selectivity. *Angew. Chem.* **2008**, *120*, 4198–4201. [CrossRef]
101. Burtch, N.C.; Jasuja, H.; Walton, K.S. Water Stability and Adsorption in Metal–Organic Frameworks. *Chem. Rev.* **2014**, *114*, 10575–10612. [CrossRef]
102. Zuluaga, S.; Fuentes-Fernandez, E.M.A.; Tan, K.; Xu, F.; Li, J.; Chabal, Y.J.; Thonhauser, T. Understanding and controlling water stability of MOF-74. *J. Mater. Chem. A* **2016**, *4*, 5176–5183. [CrossRef]
103. Li, Y.; Miao, J.; Sun, X.; Xiao, J.; Li, Y.; Wang, H.; Xia, Q.; Li, Z. Mechanochemical synthesis of Cu-BTC@GO with enhanced water stability and toluene adsorption capacity. *Chem. Eng. J.* **2016**, *298*, 191–197. [CrossRef]
104. Yang, Q.; Vaesen, S.; Ragon, F.; Wiersum, A.D.; Wu, D.; Lago, A.; Devic, T.; Martineau, C.; Taulelle, F.; Llewellyn, P.L.; et al. A water stable metal–organic framework with optimal features for CO2 capture. *Angew. Chem. Int. Ed.* **2013**, *39*, 10316–10320. [CrossRef]
105. He, T.; Kong, X.-J.; Li, J.-R. Chemically Stable Metal–Organic Frameworks: Rational Construction and Application Expansion. *Acc. Chem. Res.* **2021**, *54*, 3083–3094. [CrossRef] [PubMed]
106. Wang, K.; Huang, H.; Zhou, X.; Wang, Q.; Li, G.; Shen, H.; She, Y.; Zhong, C. Highly Chemically Stable MOFs with Trifluoromethyl Groups: Effect of Position of Trifluoromethyl Groups on Chemical Stability. *Inorg. Chem.* **2019**, *58*, 5725–5732. [CrossRef] [PubMed]
107. Liu, T.-F.; Zou, L.; Feng, D.; Chen, Y.-P.; Fordham, S.; Wang, X.; Liu, Y.; Zhou, H.-C. Stepwise Synthesis of Robust Metal–Organic Frameworks via Postsynthetic Metathesis and Oxidation of Metal Nodes in a Single-Crystal to Single-Crystal Transformation. *J. Am. Chem. Soc.* **2014**, *136*, 7813–7816. [CrossRef] [PubMed]
108. Shen, Y.; Tissot, A.; Serre, C. Recent progress on MOF-based optical sensors for VOC sensing. *Chem. Sci.* **2022**, *13*, 13978–14007. [CrossRef] [PubMed]
109. Bian, Y.; Wang, R.; Wang, S.; Yao, C.; Ren, W.; Chen, C.; Zhang, L. Metal–organic framework-based nanofiber filters for effective indoor air quality control. *J. Mater. Chem. A* **2018**, *6*, 15807–15814. [CrossRef]
110. Li, W.; Wu, X.; Han, N.; Chen, J.; Qian, X.; Deng, Y.; Tang, W.; Chen, Y. MOF-derived hierarchical hollow ZnO nanocages with enhanced low-concentration VOCs gas-sensing performance. *Sens. Actuators B Chem.* **2016**, *225*, 158–166. [CrossRef]
111. Homayoonnia, S.; Zeinali, S. Design and fabrication of capacitive nanosensor based on MOF nanoparticles as sensing layer for VOCs detection. *Sens. Actuators B Chem.* **2016**, *237*, 776–786. [CrossRef]

112. Zhang, Y.; Zhou, Y.; Li, Z.; Chen, G.; Mao, Y.; Guan, H.; Dong, C. MOFs-derived NiFe2O4 fusiformis with highly selective response to xylene. *J. Alloys Compd.* **2019**, *784*, 102–110. [CrossRef]
113. Sapsanis, C.; Omran, H.; Chernikova, V.; Shekhah, O.; Belmabkhout, Y.; Buttner, U.; Eddaoudi, M.; Salama, K.N. Insights on Capacitive Interdigitated Electrodes Coated with MOF Thin Films: Humidity and VOCs Sensing as a Case Study. *Sensors* **2015**, *15*, 18153–18166. [CrossRef] [PubMed]
114. Chen, D.-M.; Zhang, N.-N.; Liu, C.-S.; Du, M. Template-directed synthesis of a luminescent Tb-MOF material for highly selective Fe^{3+} and Al^{3+} ion detection and VOC vapor sensing. *J. Mater. Chem. C* **2017**, *5*, 2311–2317. [CrossRef]
115. Tung, T.T.; Tran, M.T.; Feller, J.-F.; Castro, M.; Van Ngo, T.; Hassan, K.; Nine, J.; Losic, D. Graphene and metal organic frameworks (MOFs) hybridization for tunable chemoresistive sensors for detection of volatile organic compounds (VOCs) biomarkers. *Carbon* **2020**, *159*, 333–344. [CrossRef]
116. Chen, H.; You, Z.; Wang, X.; Qiu, Q.; Ying, Y.; Wang, Y. An artificial olfactory sensor based on flexible metal–organic frameworks for sensing VOCs. *Chem. Eng. J.* **2022**, *446*, 137098. [CrossRef]